Biomass and Bioenergy 214 (2026) 109511

Contents lists available at ScienceDirect

Biomass and Bioenergy

journal homepage: www.elsevier.com/locate/biombioe

Green synthesis of crystalline silicon nanoparticles (SiNPs) via magnesiothermic reduction of mesoporous silica extracted from sugarcane bagasse ash (SCBA)

Lyle A. September [a,*], Ntombizonke Kheswa [b], Ntalane S. Seroka [a,c,**], Lindiwe Khotseng [a]

[a] Department of Chemistry, University of the Western Cape, Bellville, South Africa
[b] NRF/iThemba LABS (Laboratory for Accelerator Based Sciences), Old Faure Road, Faure, South Africa
[c] Energy Centre, Smart Places Cluster, Council for Scientific and Industrial Research (CSIR), Pretoria, South Africa

ARTICLE INFO

Keywords:
Crystalline silicon nanoparticles
Mesoporous silica
Green synthesis
Sugarcane bagasse ash
Magnesiothermic reduction
Low temperature
Waste valorisation

ABSTRACT

In this study, crystalline silicon nanoparticles (SiNPs) were successfully produced utilising a low-temperature magnesiothermic reduction method of mesoporous silica nanoparticles (SiO_2NPs). Silicon nanoparticles (SiNPs) have gained attention in recent years due to their range of applications and specific properties. However, producing high-purity SiNPs necessitates high-energy production, such as carbothermic reduction at >2000 °C, in addition to the significant pollutants and CO_2 emissions generated throughout the process. Thus, there has been an increase in research on extracting SiNPs from various agricultural wastes as a cost-effective source. This study investigates the extraction of SiO_2NPs using sol-gel synthesis from sugarcane bagasse ash (SCBA) and resulted in a purity of 94.8% utilising XRF. After magnesiothermic reduction of SiO_2NPs at 650 °C, XRD and Raman confirmed the resulting crystalline SiNPs. Furthermore, SEM and TEM were used to investigate the morphology along with BET to determine specific surface area, pore volume, and pore diameter, which resulted in 57.85 m^2/g, 0.18 cm^3/g, and 12.4 nm, respectively, for the produced SiNPs. Additionally, this study includes the use of a green-sustainable synthesis method to decrease energy usage and attempts to replace toxic counterparts with reagents such as the use of L-cysteine hydrochloride monohydrate and citric acid, while obtaining high-purity SiNPs. SiNPs have a variety of possible applications in new advancements, including energy production like solar photovoltaic cells and energy storage devices, which contribute towards the UN's sustainable development goals (SDG), particularly SDG 7 (Affordable and clean energy) and SDG 13 (Climate Action), as this study exhibits sustainability and increases the potential to reduce biomass waste production.

1. Introduction

The persistent pursuit of technological improvement, notably in industries such as electronics, photovoltaics, and biomedicine, has resulted in an increasing need for high-purity silicon nanoparticles [1], [2]. Crystalline silicon nanoparticles (SiNPs) are driving this demand because of their unique optoelectronic capabilities, biocompatibility, and quantum effects at the nanoscale. Crystalline silicon is a desirable material of choice for energy applications such as solar cells, lithium-ion batteries, supercapacitors and hydrogen production [3]. Silicon can be refined by employing relatively economical methods. However, traditional techniques for synthesising SiNPs, such as chemical vapour deposition and laser ablation, are frequently energy-intensive, need hazardous precursors (e.g., silane gas), and produce considerable toxic byproducts, creating severe environmental and economic problems [4], [5].

In the above-mentioned methods, SiNPs are synthesized using chemicals as a raw material. In chemical methods, it is easy to control the size, shape, and purity of the material, but the starting reagents are costly and hazardous. In industrial applications, a low cost and a large quantity of initial precursors are needed. Therefore, it is necessary to determine an alternative method for the production of SiNPs [6]. In parallel, the worldwide agriculture industries produce millions of tonnes of biomass waste each year, posing a substantial disposal concern [7]. A

This article is part of a special issue entitled: SBP2025 published in Biomass and Bioenergy.

* Corresponding author.
** Corresponding author. Department of Chemistry, University of the Western Cape, Bellville, South Africa.
E-mail addresses: 3727392@myuwc.ac.za (L.A. September), 3754640@myuwc.ac.za (N.S. Seroka).

https://doi.org/10.1016/j.biombioe.2026.109511
Received 12 January 2026; Received in revised form 28 April 2026; Accepted 28 April 2026

notable example is sugarcane bagasse ash (SCBA), a byproduct of sugar and ethanol mills that burn bagasse for electricity generation after extraction. SCBA, made mostly of amorphous silica (SiO_2), is often discarded as garbage in landfills [8]. This conflict between the requirement for sustainable nanomaterial manufacturing and the problem of agricultural waste buildup provides an important opportunity for innovation. Moreover, there are a number of agricultural wastes that can be used for the production of silica nanoparticles (SiO_2NPs), namely sugarcane bagasse, wheat husk, bamboo leaves and rice husk. Currently, rice husk is extensively researched for silica and silicon synthesis, while sugarcane bagasse remains under-explored [9].

The term "green synthesis" has developed as a paradigm change in nanomaterial research, emphasising the use of environmentally friendly reagents, renewable resources, and energy-efficient methods [10]. In this perspective, extracting silica from SCBA and converting it into value-added SiNPs is well aligned with circular economy concepts. This process not only repurposes an industrial waste product, but it also provides a cost-effective and ecologically friendly alternative to standard synthesis techniques. It consists of more than 50% amorphous silica. Therefore, it confirms that SCBA can be used as a source material for the production of SiNPs.

Currently, in the extraction of silica NPs, there are numerous methods for the purification of SCBA, including chemical and thermal treatments and other methods like sol-gel extraction. Chemical treatments like acid leaching are currently utilised in the removal of heavy metal oxides in the ash; strong acids like hydrochloric acid (HCl) and sulphuric acid (H_2SO_4) are generally used [11]. Though these acids are successful in the removal of impurities, however they are known to be detrimental to the environment and unsustainable. Recent research shows the use of more ecofriendly leaching agents, such as the use of citric acid ($C_6H_8O_7$) and L-cysteine hydrochloride monohydrate ($C_3H_{10}ClNO_3S$) [12]. While acid treatments are effective, thermal treatments (including calcination) are necessary in the elimination of carbon. These are generally paired together, as they are very effective in removing impurities in SCBA; however, they do not result in high-purity silica. Furthermore, chemical extraction methods like the sol-gel synthesis, which include the extraction of silica in the form of a sodium silicate solution through the use of sodium hydroxide (NaOH) and then following a gel formation under controlled pH utilising an acid (such as HCl) [13]. Similarly, recent studies show the use of eco-friendly reagents like citric acid and L-cystein hydrochloride monohydrate for gel formation in sol-gel synthesis. Sol-gel extraction is known to be the best alternative method for high-purity silica but is still dependent on the number of impurities in SCBA. Due to both routes being dependent on the number of impurities in SCBA, combining the chemical and thermal treatments with the sol-gel approach could result in higher purity.

Despite the availability of a number of studies on the synthesis and application of silica from natural resources, there's only a small amount of information available about silicon nanoparticle production. The reduction of silica (SiO_2) to silicon (Si) is an important stage in this process. While traditional metallurgical procedures employ carbon at extremely high temperatures (>2000 °C) [14]. Reduction is generally carried out in an electric arc furnace, with carbon and an excess of SiO_2 to stop silicon carbide (SiC) from accumulating. This reaction is known as carbothermal reduction of SiO_2. Newer breakthroughs have investigated more regulated approaches utilising environmentally friendly reducing agents like magnesium and aluminium [15]. Metallothermic reduction operations can employ manufactured and natural SiO_2 sources as feedstock to produce Si at low temperatures and in a single step. The reduction of SiO_2 with Mg is known as magnesiothermic reduction, and it is the most researched metal among the other possibilities. Currently studies show magnesiothermic reduction has been shown to yield silicon structures from silica at temperatures between 500 and 950 °C, enabling assisted design of silicon structures [16]. It is shown that higher temperatures, between 750 and 950 °C, result in superior silicon structures, as this solid-state reduction is diffusion-controlled; thus, higher temperatures and longer resident times favour the reaction. Moreover, studies relating to silica extracted from SCBA for the production of silicon involve the use of 800 °C at a short residence time [17]. To reduce energy consumption, feasibly lowering the temperature for a longer period of residence can be explored. Of all the metals that may reduce SiO_2, Mg has one of the lowest bulk melting temperatures of 650 °C and is the most volatile, having a high vapour pressure at very low temperatures, allowing quick reaction periods at relatively low temperatures [18]. Interestingly, because the reaction conditions take place at lower temperatures, the magnesiothermic reduction of silica into silicon utilises less energy than the equivalent carbothermic reduction process [19]. Applying a green reduction approach to SCBA-derived silica to produce crystalline SiNPs is a big scientific issue since it necessitates precise control of reaction kinetics and purification to obtain the appropriate phase and particle size.

As a result, this study describes a unique synthesis technique for producing crystalline SiNPs directly from sugarcane bagasse. Thus, the aim of this study was to synthesise silicon nanoparticles from silica nanoparticles produced from SCBA by magnesiothermic reduction. The paper shows a closed-loop method that starts with the extraction of high-purity silica from SCBA, utilising chemical and thermal treatment along with the sol-gel synthesis to decrease the number of impurities in silica and then a low-temperature magnesiothermic reduction procedure to generate crystalline silicon. This study not only provides a sustainable avenue for silicon production, but it also helps waste management solutions by demonstrating how agricultural waste may be transformed into technologically essential nanoparticles. Silicon nanoparticles extracted from sugarcane bagasse are an excellent candidate for applications in a variety of new technological advancements, such as nanoelectronics, energy production, and storage devices, because of their application-specific and superior properties, as well as their high surface area and small particle size [20].

2. Materials and methods

2.1. Materials

The various experiments in the present paper were carried out using analytical reagent-grade chemicals and chemical reagents that required no further purification. Sigma-Aldrich supplied 99.5% citric acid ($C_6H_8O_7$), 98% L-cysteine hydrochloride monohydrate, 98% sodium hydroxide (NaOH) and 99% magnesium (Mg) for the production of silicon dioxide and silicon. All tests utilised deionised water from the Milli-Q water purification system (Millipore, Bedford, MA, USA) in aqueous form. Sugarcane bagasse was sourced from the Illovo Sugar Company in South Africa.

2.2. Extraction of silica nanoparticles

The extraction of silica nanoparticles was adopted from September et al. [21]. To remove sand and dust particles, the bagasse ash was washed and immersed in double-deionised water for 24 h, according to conventional preparation procedures. The washed bagasse was dried, and the resultant ash was finely ground with a mill and pestle. For pretreatment, ash samples were acid-leached using a leaching agent, 5% L-cysteine hydrochloride monohydrate. To remove alkaline and alkaline earth ions, 20 g of ash was immersed in 250 mL of acidic solution in a 500 mL round-bottom flask and refluxed at 80 °C for 2 h while continuously stirring at 800 rpm. Following this, the leached ash was vacuum filtered with a Buchner funnel and 70 mm filter paper, then washed with distilled water until the pH of the decant was neutral (pH 7). Following that, the bagasse ash samples were tagged appropriately and dried overnight at 100 °C in a lab oven. In order to eliminate the carbon content found in the ash sample, the leached samples were calcined after the leaching process. The samples were heated to 700 °C, heated at a rate of 10 °C per minute, and held for 6 h in a laboratory muffle furnace

(Thermo Scientific-Thermolyne benchtop muffle furnace).

$$SiO_2(SCBA) + 2\,NaOH_{(aq)} \rightarrow Na_2SiO_{3(aq)} + H_2O \quad \text{Equation 1}$$

Silica nanoparticles were initially synthesized through the sol-gel polymeric route using industrial sugarcane bagasse ash. In a round-bottom flask with a 1:10 w/v ratio, the pre-treated ash was dissolved in 1 M NaOH; quantitatively, 10 g of pretreated ash was dissolved in 100 mL of NaOH. In order to facilitate the dissolution of silicon dioxide in the ash sample, the pre-treated ash was suspended under reflux for 1 h while being continuously stirred at 600 rpm using a magnetic stirrer at 90 °C (Equation (1)). Consequently, a solution high in sodium silicate is produced. The sodium silicate-rich solution was filtered using a Buchner funnel and 70 mm filter paper to remove ash impurities after an hour of cooling to ambient temperature.

Neutralization (balanced)

$$3\,Na_2SiO_3 + 2\,C_6H_8O_7 \rightarrow 2\,Na_3C_6H_5O_7 + 3\,H_2SiO_3 \quad \text{Equation 2}$$

After that, 5% citric acid (CA) was used to titrate the sodium silicate-rich solution, Equation (2). The Lasec pH 80+ DHS Bench Meter was used to measure the pH of the solution until it reached a pH of 7. The solution was titrated by neutralization (gelling process) under slow and continuous stirring.

Silicic acid condensation

$$3\,H_2SiO_3 \rightarrow 3\,SiO_2 + 3\,H_2O \quad \text{Equation 3}$$

Overall (with silica precipitate)

$$3\,Na_2SiO_3 + 2\,C_6H_8O_7 \rightarrow 2\,Na_3C_6H_5O_7 + 3\,SiO_2 + 3\,H_2O \quad \text{Equation 4}$$

To create a silica gel, the titrated solutions were aged for 48 h before being separated by centrifugation using the Lasec Centrifuge TG16.5. To create xerogels, the silica gel was periodically cleaned with double-deionised water and dried at 100 °C for a whole day in an oven. The white silica powder was obtained by crushing the xerogels with a mortar and pestle.

2.3. Magnesiothermic reduction

As previously described by other researchers, the use of the prepared silicon dioxide nanoparticles, which were extracted from SCBA, as a precursor for the production of silicon nanoparticles through the use of magnesiothermic reduction. The previously obtained silica nanoparticles were mixed with magnesium powder. After combining in a molar ratio of SiO_2:Mg (1:2), shown in Equation (5), the mixture was ground using a mortar and pestle to obtain a homogeneous mixture. In a tube furnace, the uniformly grounded mixture was subjected to a pyrolysis temperature of 650 °C for 4 h. The conditions for the reaction occurred under inert gas (nitrogen, N_2) with a heating rate of 10 °C/min. Post reaction, the sample was left to cool to room temperature. A brown powder is obtained; the powder sample was mixed with aqua regia (1HNO_3:3HCl) solution at room temperature for 2 h with the aim of removing magnesium oxide and/or magnesium silicate. Thereafter, it was washed with deionised water until a neutral pH was achieved and dried in an oven at 100 °C for 12 h. Lastly, the obtained powders were labelled accordingly for further characterisation.

$$SiO_2 + 2\,Mg_{(s)} \rightarrow 2\,MgO_{(s)} + Si_{(s)} \quad \text{Equation 5}$$

2.4. Characterisation

The Rigaku MiniFlex 6G benchtop X-ray diffractometer (XRD) was utilised to determine the sample's crystalline phases. The Bragg angle array has a range of $2\theta = 10–90°$ and a scanning step of 0.035°. Raman spectroscopy is used to study the molecular vibrational modes. High-performance Raman spectroscopy and spectral Raman mapping (WITec's Raman microscopy alpha300 R) were used, and the data was collected under room conditions. The sample's morphology and crystallinity were examined using transmission electron microscopy (TEM) (FEI T20 TEM). 100% ethanol was used to prepare the samples, which were then sonicated for 5 min. The samples were then drop coated onto carbon/gold-covered copper grids to make them conductive. Using the Micromeritics 3Flex high-performance gas adsorption analyser and the one-point BET/BJH technique, textural features such as specific surface area (SSA), pore volume (Vp), and pore diameter (Dp) for N_2 physisorption at 77K were examined. Every sample was examined for textural characteristics after being degassed for an entire night at 120 °C.

3. Results and discussion

As shown in Table 1, the chemical elemental composition of the raw sugarcane bagasse ash utilised, as well as the xerogel formed using the sol-gel procedures employed in the purification of SiO_2, was determined using X-ray fluorescence spectroscopy (XRF). The silica content in the raw ash displayed a weight percentage of 74.5%. Despite the silica concentration, the primary impurities contained in the ash are Fe_2O_3 and Al_2O_3 (8.66% and 4.47%, respectively). The resulting impurities present in the ash are the result of industrial operations such as harvesting, transporting and storage of bagasse ash. The other elements detected are impurities, which are expected when working with a biological waste source like sugarcane bagasse ash.

The XRF analysis confirms that the extracted product from sugarcane bagasse ash is 94.8 wt% pure SiO_2 by mass. It validates the effectiveness of the process, purification and silica extraction. The remaining 5.2% consists of trace amounts of other elements, predominantly sodium (Na) and aluminium (Al). The specific impurities act as a fingerprint that directly links the extracted silica to its SCBA origin, which is a key point in a green synthesis. The presence of these dopants, especially Al, which is a p-type dopant and can influence the electronic properties of the silica, could be an interesting point for future research or discussion. Similarly, other research on the extraction of silica from SCBA resulted in a purity of 98.92% and 96.8% for Farirai et al. (2020) and Falk et al. (2019) [17], [22], respectively, utilising HCl in the sol-gel methods. This is comparable to the resulting purity of the silica extracted in this research.

The XRD patterns for silica are presented in Fig. 1(a); the particles

Table 1
X-ray Fluorescence (XRF) of raw sugarcane bagasse ash and the extracted silica nanoparticles (SiO_2NPs).

Compound	Raw SCBA (wt%)	Silica NPs (wt%)
SiO_2	74.50	94.80
Fe_2O_3	8.66	0.09
Al_2O_3	4.47	1.05
K_2O	3.37	-
TiO_2	2.34	-
Cl	2.26	0.12
CaO	1.67	-
MgO	0.67	0.36
NbO	0.52	0.38
MoO_3	0.48	0.27
P_2O_5	0.44	0.16
SO3	0.20	-
MnO	0.11	-
Cr_2O_3	0.06	>0.01
ZnO	0.05	>0.01
NiO	0.05	0.03
SrO	0.03	-
V_2O_5	>0.03	-
Cu_2O	0.03	>0.01
Rb_2O	0.02	>0.01
Y_2O_3	0.01	-
Ga_2O_3	>0.01	>0.01
Na_2O	-	2.63
Rh_2O_3	-	0.06
Total	99.99	99.99

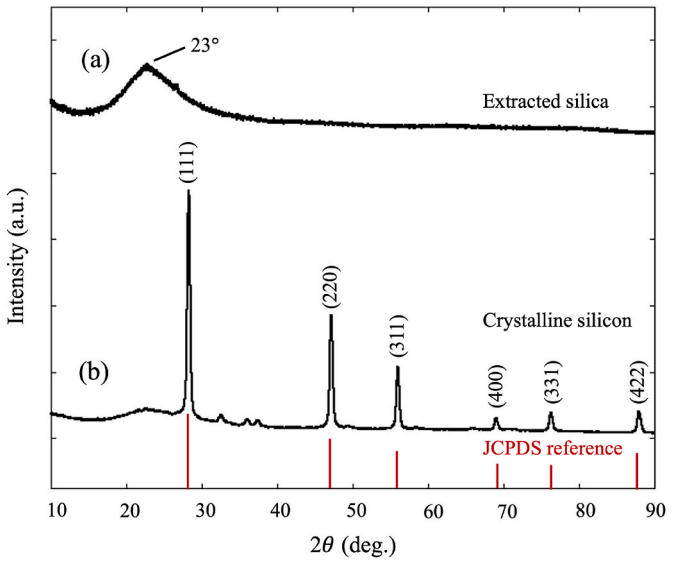

Fig. 1. XRD pattern of the extracted (a) SiO_2 using sol-gel synthesis and (b) silicon through magnesiothermic reduction at 650 °C. The XRD pattern for crystalline silicon reference (JCPDS) (red lines), indicating the expected line position. (For interpretation of the references to colour in this figure legend, the reader is referred to the Web version of this article.)

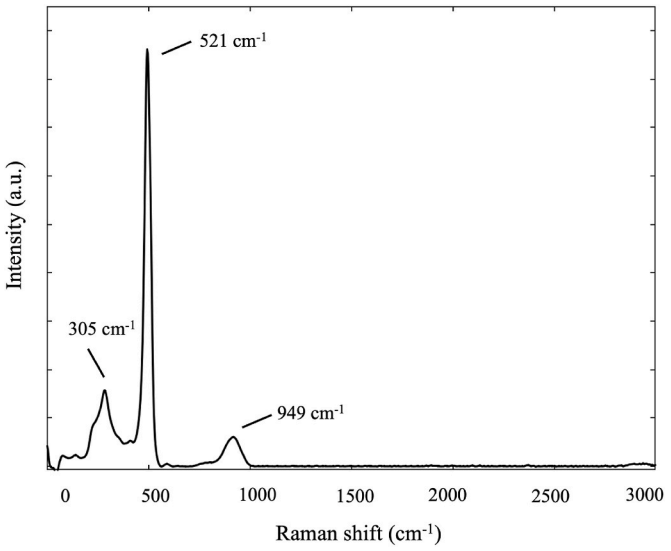

Fig. 2. Raman spectrum of SiNPs extracted from sugarcane bagasse ash via magnesiothermic reduction of silica at 650 °C.

exhibit a pattern of amorphous silica, a broad peak at 23°. In actuality, burning an organic material with a high silicon content, such as sugarcane waste, can result in the formation of either crystalline or amorphous silica. Crystalline silica is typically produced at temperatures between 900 and 1000 °C, where crystals form. Fig. 1(b) displays the X-ray diffraction (XRD) pattern for silicon nanoparticles. Based on the peak locations and intensity, the figure shows a traditional and excellent diffraction pattern. The pattern clearly corresponds to a highly crystalline cubic (diamond-cubic) silicon material. The distinctive "fingerprint" of crystalline silicon is shown by the three most noticeable peaks: peak values of around 28.4°, 47.3°, and 56.1° correspond to the (111), (220), and (311) planes, respectively. Since the (111) plane is the most densely packed, it is the most intense peak, which is usual for silicon. The background signal (or "noise") is low, and the peaks are powerful and sharp. This suggests that the material's atomic structure is well organised across extended distances, indicating that it is well crystallised. The pattern shows no further notable peaks, indicating the successful reduction of silica to silicon. With the exception of the potential unreacted silica, SiO_2, which is shown by a large hump at about 22–23°, this indicates that the synthesized material is pure silicon with no discernible crystalline imperfections. Based on the 2θ of the Scherrer Equation estimates the crystallite size to be 21 nm for Si. Falk et al. (2019) [17] provided support for this work by synthesising silicon nanoparticles from sugarcane bagasse ash using magnesiothermic reduction.

Fig. 2 displays the Raman spectrum of the extracted silicon nanoparticles. A main Raman peak was detected around 500 cm^{-1}. This resulted from the scattering of the silicon NPs first-order optical phonon. A peak at 521 cm^{-1} was noted in their analysis of the crystalline silicon Raman spectra. This spectrum is dominated by a single, sharp and intense peak; this perfectly corroborates the sharp peaks observed in the XRD pattern for highly crystalline silicon. The scattering of two transverse acoustic and two transverse optical phonons is also responsible for the two peaks at 300 cm^{-1} and 900 cm^{-1}, respectively [23]. The stretching mode of amorphous Si-Si was responsible for the modest peak centred at 949 cm^{-1}, whereas the Si–Si stretching mode was linked to the intense band of Si at 520 cm^{-1} [17].

Fig. 3 displays the SEM evaluation of the silica and silicon nanoparticles' morphology following the magnesiothermic reduction procedure. Fig. 3A shows irregular-sized particles with a smooth and soft-like surface of the extracted silica xerogel, with the EDS illustrating the presence of silicon, oxygen and carbon. The presence of carbon is highly due to the carbon tape utilised during analysis. The size and shape of the silicon nanoparticles were assessed using SEM, as shown in Fig. 3(B). All silicon powders are found to share a comparable shape to that of the silica nanoparticles synthesized. According to the SEM micrographs, both samples' particles are clumped together and form an agglomeration, similarly reported by Lai et al. [15]. Accordingly, silicon nanoparticles are used in applications where purity is crucial, such as in the fabrication of solar cells. Sugarcane bagasse ash can serve as a source of silicon nanoparticles for this particular application since the synthesized silicon's purity is high purity with a few impurities.

Fig. 4 depicts the transmission electron microscopy (TEM) images of the extracted silica nanoparticles from sugarcane bagasse ash and reduced silicon nanoparticles. In Fig. 4(A, a) typical connected three-dimensional array of nanoparticles generated by the sol-gel is visible. The SiO_2 nanoparticles show a non-uniform size and a highly agglomerated state, which is due to the gel drying process, in which the destabilization of the process favours the agglomerated state. Similarly, in Fig. 4 B, the silicon nanoparticles are agglomerated with an increase in size, decreasing the surface area of the nanoparticles. The size of the particles is circular and irregular, showing a change in the morphology of the crystalline particles of silicon. The size ranges from several nanometres to ~ 24 nm. However, no definite shape is seen for both synthesized nanoparticles, though it can be shown that they do not contain nanoparticles larger than 50 nm.

Fig. 5 shows the nitrogen physisorption of the extracted silica nanoparticles and the reduced silicon nanoparticles. Using the N_2 adsorption-desorption method, the textural characteristics of silica and silicon were assessed, and the findings are compiled in Table 2. Fig. 5 *(top)* displays the N_2 adsorption/desorption isotherms of the silica NPs made using the sol-gel method. The isotherms for the produced materials showed a type IV behaviour, which is the definitive signature of mesoporous material with pore diameters between 2 and 50 nm, and are comparable to those of porous solids. BET analysis confirmed that the SCBA-derived silica possesses a high specific surface area of 569.08 m^2/g and a Type IV isotherm with an H2 hysteresis loop, characteristic of a mesopore structure with a narrow pore size distribution. With the pore volume and pore diameter for silica being 0.64 cm^3/g, and 5.4 nm, the pore size distribution was ascertained by BJH. As a result, the materials produced using sol-gel exhibit a higher potential for application as

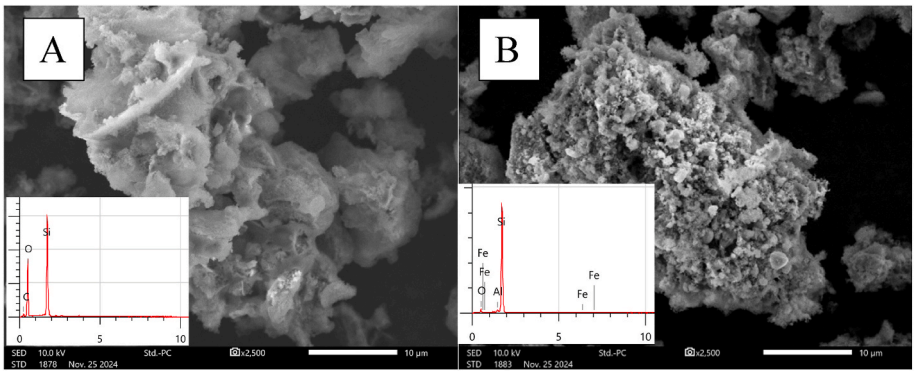

Fig. 3. SEM micrographs and EDS graph of (A) SiO_2 and (B) silicon. (For interpretation of the references to colour in this figure legend, the reader is referred to the Web version of this article.)

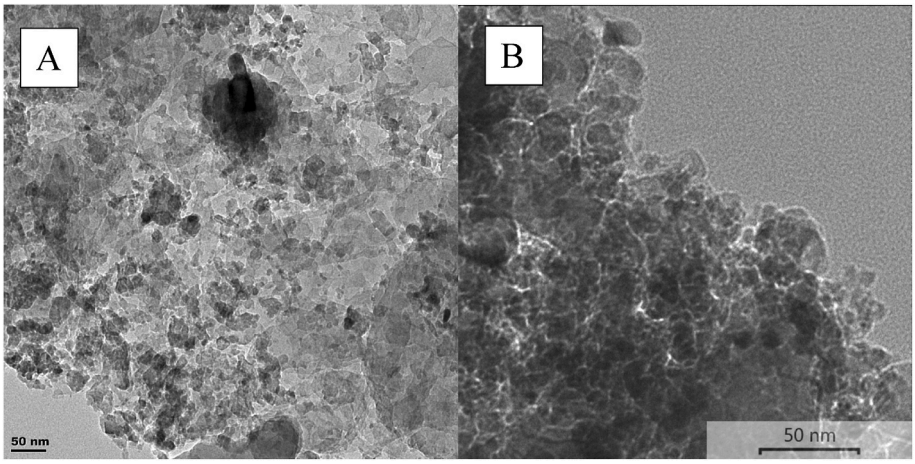

Fig. 4. TEM images of (A) SiO_2 nanoparticles prepared by the sol-gel method and (B) Si nanoparticles after magnesiothermic reduction.

adsorbents. In these circumstances, the sample made using sol-gel is mostly regarded as the synthesis of mesoporous materials.

In Fig. 5, there's a clear structural transformation, illustrating the reduction process from silica to silicon, which has caused a complete collapse of the mesoporous network. The BET specific surface area, pore volume, and pore diameter for silicon are 57,85 m^2/g, 0,18 cm^3/g, and 12,4 nm. The high-surface-area, porous framework of silica precursor has been transformed into a dense, non-porous material. At the lower P/P_0 areas, the amount of adsorbed gas steadily rises as P/P_0 increases. The hysteresis loop is seen for the Si isotherm at a range of $0,4 < P/P_0 < 1,0$, which is linked to capillary condensation occurring in the mesopores [24]. The most direct observation is the decrease in the quantity adsorbed when compared to the silica isotherm, which is well over 200 cm^3/g.

The final product's BET analysis verified the anticipated structural change that occurred during the magnesiothermic reduction. The Type IV isotherm changed to a Type II isotherm, and the specific surface area significantly decreased with an increase in pore diameter, indicating that the high-surface-area mesoporous silica precursor was transformed into dense, non-porous silicon nanoparticles. The production of the crystalline silicon phase seen in XRD and Raman measurements is consistent with this densification.

4. Conclusion

The findings in this current research demonstrate the efficiency of the sustainable procedure described for the production of crystalline silicon NPs from sugarcane bagasse ash-derived silica NPs by use of the magnesiothermic reduction method. The recovered silica from sugarcane bagasse ash (SCBA) was successfully used to produce the silicon nanoparticles. The study effectively closes the loop on waste valorisation by converting a low-value residue into a high-value nanomaterial, which is completely consistent with the concepts of green chemistry and circular economy. Quantitative elemental composition and physical properties of the silicon nanoparticles produced.

BET analysis indicated that SCBA had high-surface-area, mesoporous silica. The silica precursor was converted to elemental silicon by a solid-state reaction, resulting in a basic chemical change from SiO_2 to Si. The final product's BET analysis verified the anticipated structural change that occurred during the magnesiothermic reduction. The Type IV isotherm changed to a Type II isotherm, and the specific surface area significantly decreased. X-ray Diffraction (XRD) revealed crystalline silicon peaks and Raman spectroscopy confirmed the presence of a strong phonon mode at $\sim 520\ cm^{-1}$. The resultant material has excellent crystallinity and phase purity.

Furthermore, these findings demonstrated that a sustainable source of silica can be used to produce silicon nanoparticles. Megnesiothermic reduction is effective and a stable process, and it can compete with a traditional carbothermal reduction process. In conclusion, this work establishes a viable and innovative green synthesis route for silicon nanoparticles. It not only addresses the management of sugarcane bagasse ash, but it also provides a cost-effective and ecologically friendly alternative to traditional approaches that rely on energy-intensive procedures and hazardous precursors. This study presents a proof-of-concept for a green synthesis method; nonetheless, we recognise that a thorough life-cycle evaluation and a comprehensive mass/energy

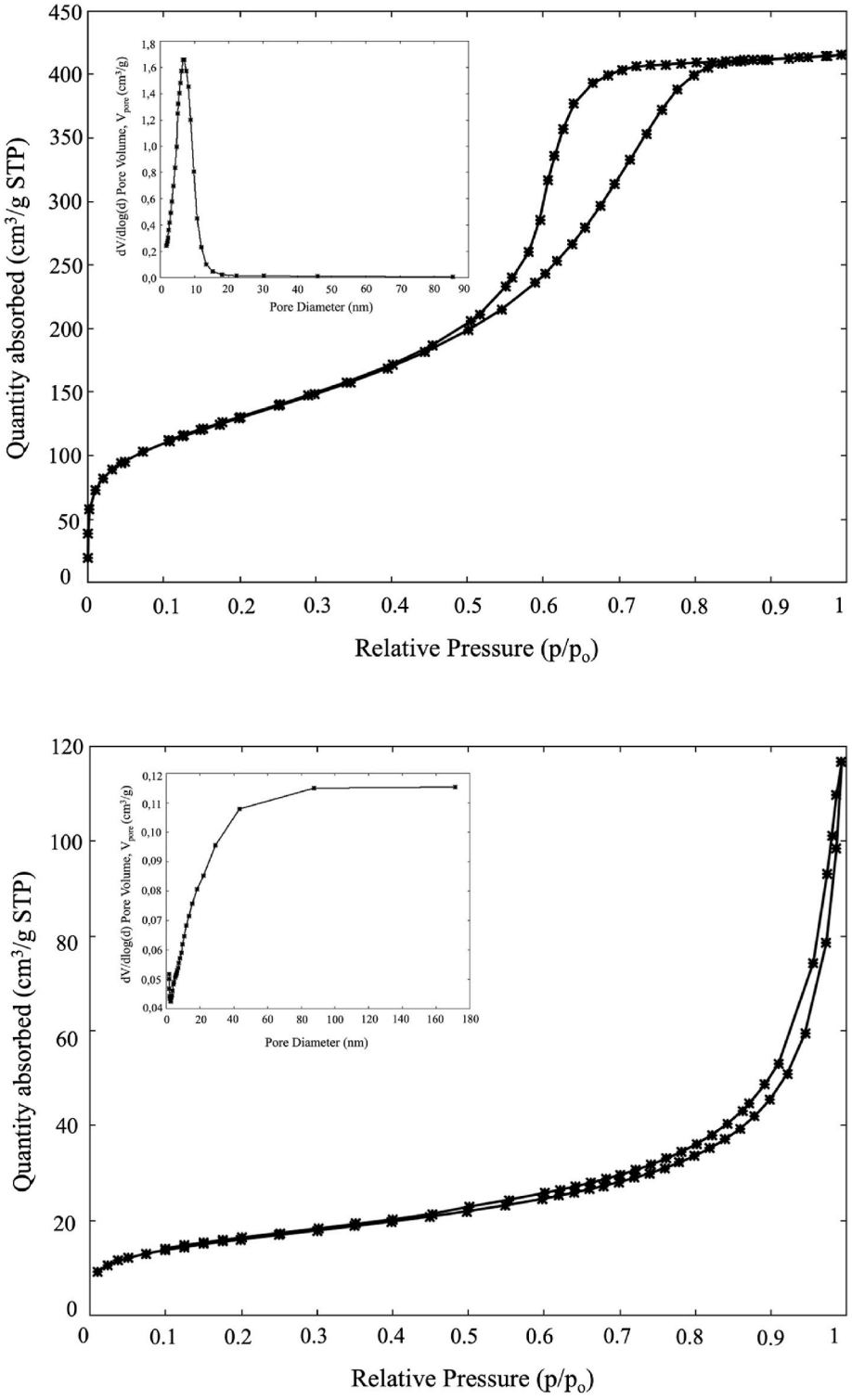

Fig. 5. BET isotherm for the extracted SiO_2 nanoparticles *(top)* and Si nanoparticles *(bottom)*.

Table 2
BET summary of SiNPs extracted from SCBA.

	BET Surface Area (m^2/g)	V_{pore} (cm^3/g)	d_{pore} (Å)	$width_{pore}$ (Å)
Raw SCBA	59.68	0.09	-	62.34
Silica NPs	469.08	0.64	54.74	46.74
Silicon NPs	57.85	0.18	124.67	128.7

balance are essential to validate the environmental and economic claims. The high-quality SiNPs created have great potential for use in a variety of industries, including electronics, photovoltaics, and energy storage. Future research will concentrate on optimising the reduction process to achieve exact control over particle size and assessing the efficacy of these SiNPs in specific applications, such as anodes for lithium-ion batteries.

Funding

This research was funded by the National Research Foundation (South Africa): 138079 and Eskom (South Africa): 2002/015527/0.

CRediT authorship contribution statement

Lyle A. September: Investigation, Methodology, Writing – original draft, Writing – review & editing. **Ntombizonke Kheswa:** Conceptualization, Data curation, Resources. **Ntalane S. Seroka:** Formal analysis, Investigation, Methodology, Visualization, Writing – review & editing. **Lindiwe Khotseng:** Project administration, Resources, Supervision.

Conflicts of interest

The authors declare no conflicts of interest.

Appendix A. Supplementary data

Supplementary data to this article can be found online at https://doi.org/10.1016/j.biombioe.2026.109511.

Data availability

Data will be made available on request.

References

[1] A. Boretti, S. Castelletto, Silicon nanoparticles in energy storage: advances, challenges, and future perspectives, Silicon 17 (8) (Jun. 2025) 1799–1810, https://doi.org/10.1007/s12633-025-03308-5.
[2] L. Chen, et al., Silicon-containing nanomedicine and biomaterials: materials chemistry, multi-dimensional design, and biomedical application, Chem. Soc. Rev. 53 (3) (2024) 1167–1315, https://doi.org/10.1039/D1CS01022K.
[3] T. Ingsel, R.K. Gupta, Nanostructured silicon for energy applications, in: Silicon-Based Hybrid Nanoparticles, Elsevier, 2022, pp. 169–197, https://doi.org/10.1016/B978-0-12-824007-6.00015-0.
[4] F. Farirai, et al., Methods of extracting silica and silicon from agricultural waste ashes and application of the produced silicon in solar cells: a mini-review, Int. J. Sustain. Eng. 14 (1) (Jan. 2021) 57–78, https://doi.org/10.1080/19397038.2020.1720854.
[5] T. Kim, J. Lee, Silicon nanoparticles: fabrication, characterization, application and perspectives, Micro and Nano Systems Letters 11 (1) (Nov. 2023) 18, https://doi.org/10.1186/s40486-023-00184-9.
[6] N.S. Seroka, R.T. Taziwa, L. Khotseng, Extraction and synthesis of silicon nanoparticles (SiNPs) from sugarcane bagasse ash: a mini-review, Applied Sciences 12 (5) (Feb. 2022) 2310, https://doi.org/10.3390/app12052310.
[7] I.-M. Toplicean, A.-D. Datcu, An overview on bioeconomy in agricultural sector, biomass production, recycling methods, and circular economy considerations, Agriculture 14 (7) (Jul. 2024) 1143, https://doi.org/10.3390/agriculture14071143.
[8] Q. Xu, T. Ji, S.-J. Gao, Z. Yang, N. Wu, Characteristics and applications of sugar cane bagasse ash waste in cementitious materials, Materials 12 (1) (Dec. 2018) 39, https://doi.org/10.3390/ma12010039.
[9] L.A. September, N. Kheswa, N.S. Seroka, L. Khotseng, Green synthesis of silica and silicon from agricultural residue sugarcane bagasse ash – a mini review, RSC Adv. 13 (2) (2023) 1370–1380, https://doi.org/10.1039/D2RA07490G.
[10] R. Saxena, et al., A review on green synthesis of nanoparticles toward sustainable environment, Sustain. Chem. Clim. Action 6 (Jun. 2025) 100071, https://doi.org/10.1016/j.scca.2025.100071.
[11] C.P. Faizul, C. Abdullah, B. Fazlul, Review of extraction of silica from agricultural wastes using acid leaching treatment, Adv. Mater. Res. 626 (Dec. 2012) 997–1000. https://doi.org/10.4028/www.scientific.net/AMR.626.997.
[12] N.S. Seroka, R. Taziwa, L. Khotseng, Green synthesis of crystalline silica from sugarcane bagasse ash: physico-chemical properties, Nanomaterials 12 (13) (Jun. 2022) 2184, https://doi.org/10.3390/nano12132184.
[13] I. Zuwanna, M. Riza, S. Aprilia, The impact of solvent concentration on the characteristic of silica from rice husk ash using sol gel method, IOP Conf. Ser. Mater. Sci. Eng. 1087 (1) (Feb. 2021) 012060, https://doi.org/10.1088/1757-899X/1087/1/012060.
[14] H.-C. Lee, et al., A simulation study on the direct carbothermal reduction of SiO2 for Si metal, Curr. Appl. Phys. 10 (2) (Mar. 2010) S218–S221, https://doi.org/10.1016/j.cap.2009.11.053.
[15] Y. Lai, J.R. Thompson, M. Dasog, Metallothermic reduction of silica nanoparticles to porous silicon for drug delivery using new and existing reductants, Chem. Eur J. 24 (31) (Jun. 2018) 7913–7920, https://doi.org/10.1002/chem.201705818.
[16] J. Entwistle, A. Rennie, S. Patwardhan, A review of magnesiothermic reduction of silica to porous silicon for lithium-ion battery applications and beyond, Royal Society of Chemistry (2018), https://doi.org/10.1039/c8ta06370b.
[17] G. Falk, G.P. Shinhe, L.B. Teixeira, E.G. Moraes, A.P.N. de Oliveira, Synthesis of silica nanoparticles from sugarcane bagasse ash and nano-silicon via magnesiothermic reactions, Ceram. Int. 45 (17) (Dec. 2019) 21618–21624, https://doi.org/10.1016/j.ceramint.2019.07.157.
[18] M. Yan, S. Martell, S.V. Patwardhan, M. Dasog, Key developments in magnesiothermic reduction of silica: insights into reactivity and future prospects, Chem. Sci. 15 (39) (2024) 15954–15967, https://doi.org/10.1039/D4SC04065A.
[19] F. Farirai, et al., Methods of extracting silica and silicon from agricultural waste ashes and application of the produced silicon in solar cells: a mini-review, Int. J. Sustain. Eng. 14 (1) (2021) 57–78, https://doi.org/10.1080/19397038.2020.1720854.
[20] T. Kim, J. Lee, Silicon nanoparticles: fabrication, characterization, application and perspectives, Micro and Nano Systems Letters 11 (1) (2023) 18, https://doi.org/10.1186/s40486-023-00184-9.
[21] L.A. September, N. Kheswa, N.S. Seroka, L. Khotseng, Green synthesis of amorphous silica nanoparticles (SiO2NPs) from sugarcane bagasse ash by sol-gel method, Next Mater. 10 (Jan. 2026) 101396, https://doi.org/10.1016/j.nxmate.2025.101396.
[22] F. Farirai, M. Mupa, M.O. Daramola, An improved method for the production of high purity silica from sugarcane bagasse ash obtained from a bioethanol plant boiler, Part. Sci. Technol. 39 (2) (2021) 252–259, https://doi.org/10.1080/02726351.2020.1734700.
[23] J.L. Liu, J. Wan, Z.M. Jiang, A. Khitun, K.L. Wang, D.P. Yu, Optical phonons in self-assembled Ge quantum dot superlattices: strain relaxation effects, J. Appl. Phys. 92 (11) (Dec. 2002) 6804–6808, https://doi.org/10.1063/1.1518756.
[24] T. Horikawa, D.D. Do, D. Nicholson, Capillary condensation of adsorbates in porous materials, Adv. Colloid Interface Sci. 169 (1) (Nov. 2011) 40–58, https://doi.org/10.1016/j.cis.2011.08.003.